

## Necklace-like Chains of Hybrid Nanospheres Consisting of Pd Nanocrystals and Peptidic Lipids

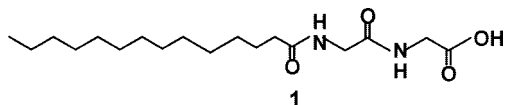
Yong Zhou,<sup>†,§</sup> Masaki Kogiso,<sup>‡,#</sup> and Toshimi Shimizu<sup>\*,†,‡,#</sup>

*SORST, Japan Science and Technology Agency (JST), Tsukuba Central 5, 1-1-1 Higashi, Tsukuba, Ibaraki 305-8565, Japan, and Nanoarchitectonics Research Center (NARC), National Institute of Advanced Industrial Science and Technology (AIST), Tsukuba Central 5, 1-1-1 Higashi, Tsukuba, Ibaraki 305-8565, Japan*

Received December 13, 2008; E-mail: tshzmz-shimizu@aist.go.jp

Use of nanocrystals (NCs) as building blocks for the fabrication of multifunctional mesoscale assemblies may create an opportunity to manufacture materials with new physical, chemical, and mechanical properties based on their collective properties. Precise control of one-dimensional (1-D) assembly of NCs can lead to applications in optical and electronic nanodevices.<sup>1</sup> Ordered 1-D chainlike assemblies of single NCs have been widely created by using crystal step edges,<sup>2</sup> crystallographic orientation,<sup>3</sup> intrinsic magnetic,<sup>4</sup> electric dipoles,<sup>5</sup> solvent-mediated self-assembly,<sup>6</sup> and 1-D hard templates such as DNA<sup>7</sup> and organic scaffolds,<sup>8</sup> and so on. However, it is still a challenge to construct 1-D chains consisting of structurally intricate units.<sup>9</sup>

In liquid media, lipid molecules self-assemble into diverse aggregate morphologies, depending on their molecular shapes and solution conditions such as lipid concentration, electrolyte concentration, pH, and temperature.<sup>10</sup> We have designed a number of lipid molecules that can self-assemble into open-ended, hollow cylindrical structures composed of rolled-up bilayer membrane walls,<sup>10,11</sup> and applied them as promising templates to create unique 1-D nanostructures,<sup>12</sup> such as one-dimensional and helical arrays of semiconductor NCs,<sup>13</sup> fluorescent and antimicrobial hybrid nanotubes,<sup>14</sup> and arrayed nanocables.<sup>15</sup>



Herein we report one-pot, high yield formation of unprecedented 1-D necklace-like chains consisting of hybrid Pd NCs embedded in spheres of a peptidic lipid. We employed the synthetic peptidic lipid, 2-(2-tetradecanamidoacetamido)acetic acid (**1**). We found that in the presence of palladium acetate [Pd(OAc)<sub>2</sub>] **1** can self-assemble into structured spheres which connect each other one-by-one to form necklace-like chains in ethanol solutions by coordination of negatively charged carboxylic (COO<sup>-</sup>) groups with Pd<sup>II</sup>. Upon reduction of ethanol, the coordinated Pd<sup>II</sup> are reduced into Pd atoms, which subsequently initiate the generation of Pd nuclei, and finally grow into Pd NCs embedded in the sphere chain of **1**. The potential applications of these necklaces include heterojunction-like structures for functional nanodevices.

The preparation procedure was described in Supporting Information. The product is dominantly (>95%) necklace-like chain architectures composed of the hybrid spheres. Those spheres with average diameters of 30–40 nm closely connect one-by-one to form 1-D chains with lengths ranging from hundreds of nanometers to

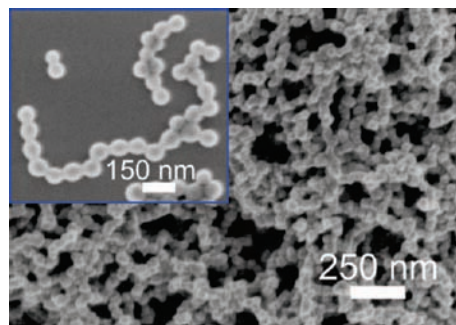


**Figure 1.** FE-SEM image of the necklace-like chains of hybrid spheres.

several micrometers. No other Pd-lipid structures were observed, demonstrating the high yield formation of the chains. A typical high-magnification field-emission scanning electron microscopic (FESEM) image shows the smooth surface of the chain (Figure 1). We found that the electron beam with acceleration voltage of 30 kV on scanning transmission electronic microscopy (STEM) cannot transmit the spherical chain, indicating that the interior of the sphere encapsulated considerable Pd NCs. Indeed, the corresponding energy dispersive X-ray (EDX) verified the Pd compositional profiles. The elemental mapping image revealed the exact composition of Pd. To reveal the incorporated Pd NCs clearly, we used TEM with acceleration voltage of 200 kV, at which the lipid moiety has very light image contrast and cannot be seen in the TEM image. The TEM image shows that well-defined, discrete Pd NC aggregates of 30–40 nm in diameter were observed. Each spherical aggregate is composed of 1–10 small Pd NCs with average diameters of 4–5 nm (Figure 2). The clear ring of the corresponding selected area electronic diffraction (SAED) pattern proves high nanocrystallinity of the Pd NCs. The high-resolution TEM (HRTEM) image of the individual Pd NC shows the lattice fringe of  $d = 2.23 \text{ \AA}$ , corresponding to the (111) crystal plane of a face-centered-cubic (fcc) Pd phase [reported  $d_{(111)} = 2.21 \text{ \AA}$ , JCPDS card file 10-454].<sup>16</sup> The wide-angle X-ray diffraction (WAXRD) pattern also confirms four diffraction peaks assignable to the (111), (200), and (220)

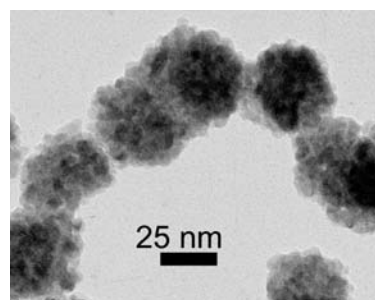


**Figure 2.** TEM image of the necklace-like hybrid chains.

<sup>†</sup> SORST, JST.

<sup>‡</sup> NARC, AIST.

<sup>#</sup> Current address: Nanotube Research Center, AIST.

<sup>\*</sup> Current address: Department of Chemistry, National University of Singapore, Singapore.

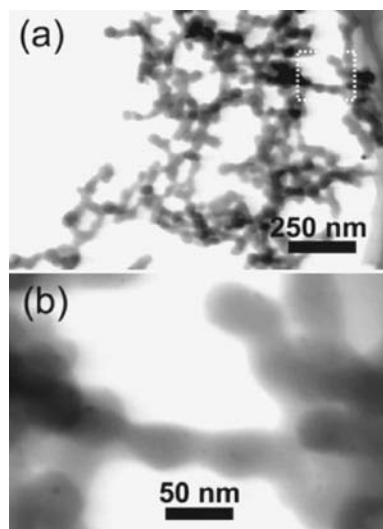


**Figure 3.** STEM images of (a) the intermediates of the necklace-like chains after cooling down for 30 min and (b) the magnified image of the selected area in panel a.

reflections of the Pd fcc phase. Typical UV–vis absorption spectra show that an ethanol solution of Pd(OAc)<sub>2</sub> gives an absorption peak at around 400 nm. This peak disappears in the obtained hybrid chains, displaying continuous absorption across the range, in good agreement with the theoretical calculations based on Mie theory.<sup>17</sup> The small angle XRD pattern of the hybrid chain shows no apparent diffraction peaks, indicating that **1** disorderly arranged in the sphere.

Synergistic effect of **1** and Pd<sup>II</sup> plays a key role in the formation of the necklace-like chain. Under the same conditions with the exception of the absence of Pd<sup>II</sup>, **1** assembles into tubular structures in ethanol solution.<sup>18</sup> In ethanol, **1** may also coordinate to a series of transit metal ions (M<sup>n+</sup>) such as Cu<sup>II</sup>, Mn<sup>II</sup>, and Ag<sup>I</sup> to form metal-complexed lipid nanotubes.<sup>18</sup> Meanwhile, in the absence of **1**, reduction of Pd(OAc)<sub>2</sub> by ethanol produced a disordered aggregate of Pd NCs. To understand the formation process of the necklace-like chain, we trapped intermediate states of the product. We found that instead of the formation of common tubular or sheet-like structures, **1** assembled into solid spheres that connect each other one-by-one via coordination with Pd<sup>II</sup> (Figure 3). The P1 process in Figure 4 schematically shows a plausible formation step of the chainlike assembly of the hybrid spheres. To the best of our knowledge, this unique spherical chain structure has never been reported among lipid assemblies. Although the exact reason why the spheres tend to align one-by-one is unknown at this moment, we believe that the balance between minimization of the surface energy and the polar repulse force among the spheres may be responsible for

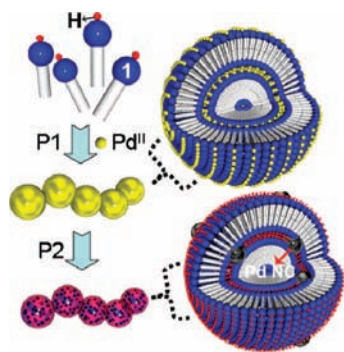


**Figure 4.** A schematic illustration for the proposed formation process of the necklace-like chains. For simplification of the image, **1** was drawn to arrange systematically in the sphere.

it, that is, the former induces the aggregation of the spheres; the latter regulates the process not randomly and intensely but systematically one by one. With aging time, the complexed Pd<sup>II</sup> ions were gradually reduced into Pd atoms by ethanol, which nucleate, eventually generating Pd NCs embedded in all over the spheres of **1** (P2 in Figure 4). Fourier-transform infrared spectroscopy should suggest that the coordination of Pd<sup>II</sup> to **1** allows the band of the carboxylic acid of **1** to disappear, and instead the band for the COO–Pd species to appear in the intermediate. However, we were unable to detect it. In the present case, the reduction of Pd<sup>II</sup> to Pd element proved to take place rapidly. Therefore, unlike other metal ion (Cu<sup>2+</sup>, Cd<sup>2+</sup>, Mn<sup>2+</sup>)–**1** complexes,<sup>18</sup> the pure Pd<sup>II</sup>–**1** complex will be difficult to be isolated as the intermediate.

Calcination of the necklace-like hybrid chains in nitrogen gas at 500 °C for 6 h allows us to carbonize the organic moiety and get the Pd-carbon nanocomposites. The necklace-like architecture was found to be preserved well although the spherical surface became rough. The application of the novel carbon/Pd 1-D nanostructure in fuel cells will be explored.

The molar ratio of the COOH of **1** to the Pd<sup>II</sup> was found to greatly affect the morphology of the products. The necklace hybrid chains can still be obtained in the case of the ratio of 4. An increase in the ratio to 8 resulted in part of disordered aggregation of Pd NCs besides the necklace chain. In addition, most of **1** self-assembled into large nanosheets. With further increase in the ratio to 16, only random Pd NCs and nanosheets of **1** were observed. Detailed reasons for the ratio of –COOH to Pd<sup>II</sup>-related hybrid nanostructures is under investigation and will be reported elsewhere.

In summary, well-defined hybrid necklace chains consisting of Pd NCs embedded in spheres of peptidic lipids have been prepared in high yields. Synergistic effect of **1** and Pd<sup>II</sup> plays a key role in the formation of the hybrid chain. The molar ratio of the –COOH of **1** to the Pd<sup>II</sup> was found to greatly affect the morphology of the products.

**Acknowledgment.** Dr. Yoshiki Shimizu (AIST) is acknowledged for HRTEM measurements.

**Supporting Information Available:** Preparation process, additional FE-SEM, STEM, TEM, and HRTEM images, and EDX, WAXRD, and UV–vis absorption spectral data. This material is available free of charge via the Internet at <http://pubs.acs.org>.

## References

- (1) Tang, Z. Y.; Kotov, N. A. *Adv. Mater.* **2005**, *17*, 951.
- (2) Zach, M. P.; Ng, K. H.; Penner, R. M. *Science* **2000**, *290*, 2120.
- (3) (a) Penn, R. L.; Banfield, J. F. *Science* **1998**, *281*, 969. (b) Banfield, J. F.; Welch, S. A.; Zhang, H.; Ebert, T. T.; Penn, R. L. *Science* **2000**, *289*, 751.
- (4) Lalatonne, Y.; Richardi, J.; Pileni, M. P. *Nat. Mater.* **2004**, *3*, 121.
- (5) Tang, Z.; Kotov, N. A.; Giersig, M. *Science* **2002**, *297*, 237.
- (6) Zhou, Y.; Antonietti, M. *J. Am. Chem. Soc.* **2003**, *125*, 14960.
- (7) (a) Deng, Z.; Tian, Y.; Lee, S. H.; Ribbe, A. E.; Mao, C. *Angew. Chem., Int. Ed.* **2005**, *44*, 3582. (b) Aldaye, F. A.; Sleiman, H. F. *Angew. Chem., Int. Ed.* **2006**, *45*, 2204.
- (8) van Bommel, K. J. C.; Friggeri, A.; Shinkai, S. *Angew. Chem., Int. Ed.* **2003**, *42*, 980.
- (9) Zhan, Y. J.; Yu, S. H. *J. Am. Chem. Soc.* **2008**, *130*, 5650.
- (10) Shimizu, T.; Masuda, M.; Minamikawa, H. *Chem. Rev.* **2005**, *105*, 1401.
- (11) Shimizu, T.; Kogiso, M.; Masuda, M. *Nature* **1996**, *383*, 487.
- (12) Zhou, Y.; Shimizu, T. *Chem. Mater.* **2008**, *20*, 625.
- (13) (a) Zhou, Y.; Ji, Q.; Masuda, M.; Kamiya, S.; Shimizu, T. *Chem. Mater.* **2006**, *18*, 403. (b) Zhou, Y.; Ji, Q.; Shimizu, Y.; Koshizaki, N.; Shimizu, T. *J. Phys. Chem. C* **2008**, *112*, 18412.
- (14) (a) Zhou, Y.; Kogiso, M.; He, C.; Shimizu, Y.; Koshizaki, N.; Shimizu, T. *Adv. Mater.* **2007**, *19*, 1055. (b) Zhou, Y.; Kogiso, M.; Asakawa, M.; Dong, S.; Kiyama, R.; Shimizu, T. *Adv. Mater.* **2009**, in press.
- (15) Zhou, Y.; Kamiya, S.; Minamikawa, H.; Shimizu, T. *Adv. Mater.* **2007**, *19*, 4194.
- (16) The Joint Committee on Powder Diffraction Standards (JCPDS)–International Centre for Diffraction Data (ICDD).
- (17) Creighton, J. A.; Eadon, D. G. *J. Chem. Soc., Faraday Trans.* **1991**, *87*, 3881.
- (18) Kogiso, M.; Zhou, Y.; Shimizu, T. *Adv. Mater.* **2007**, *19*, 242.

JA809728C